IEEE Journal of Microwaves

Received 10 August 2024; revised 2 September 2024; accepted 3 September 2024. Date of publication 2 October 2024; date of current version 2 December 2024.

Digital Object Identifier 10.1109/JMW.2024.3459859

Transmitarrays for Wireless Power Transfer on Earth and in Space

JESSE BRUNET [1] (Member, IEEE), ALEX AYLING [1] (Member, IEEE), AND ALI HAJIMIRI [1] (Fellow, IEEE)

(Invited Paper)

[1]Department of Electrical Engineering, California Institute of Technology, Pasadena, CA 91125 USA

CORRESPONDING AUTHOR: Jesse Brunet (e-mail: brunet@alumni.caltech.edu).

This work was supported by the Caltech Space Solar Power Project.

ABSTRACT We present a space solar power system using transmitarrays for lowering the system's LCOE (Levelized Cost of Energy). We discuss the theoretical framework for transmitarrays in the context of wireless power transfer, including the transmission phase limit associated with layered frequency selective surfaces. We then present a proposal for using transmitarrays to lower the LCOE of space solar powered systems that are limited by the transmitting aperture size. Finally, we design and fabricate a low-cost, lightweight static transmitarray prototype and demonstrate a $\sim$2.4x increase in power transferred from the phased array transmitter to the rectenna receiver.

INDEX TERMS Aperture coupled antenna, flexible phased array, Fourier optics, frequency selective surface, Fresnel diffraction, metasurface, microwaves in climate change, RF lens, space solar power, transmitarray, wireless power transfer.

I. INTRODUCTION

Wireless power transfer at a distance (WPT-AD) has significant potential to enable applications where physical connections are too costly, mechanically impractical, or otherwise challenging to implement. These include systems operating on both Earth [1], [2], [3], [4], [5], [6] and in space [7], [8]. Space solar power [7], [8], [9], [10], [11], [12], [13], [14], [15], [16], [17], [18], [19], [20] is promising as an alternative source of clean energy that can help address the growing challenges caused by climate change. The space solar power concept, first proposed by Isaac Asimov in his short story, "Reason" [21], envisions a solar power station in orbit around the Earth, unaffected by day/night cycles or inclement weather and having nearly 24/7 access to sunlight year-round. Caltech's proposed implementation consists of a planar, sheet-like power station coated with flexible photovoltaics that uses a microwave phased array to beam the collected power to Earth [22]. Because the microwave regime is minimally effected by the atmosphere[1] the power station can efficiently beam power regardless of weather conditions, providing clean solar power to places where traditional solar power would be impractical. A further advantage afforded by the electronically-controlled phased array architecture is that power can be dynamically and concurrently dispatched to different locations as demand requires with the ability to adjust power allocation in real time. Notably, these locations can include regions that are difficult to reach using traditional power infrastructure.

The most significant challenge when designing long distance wireless power transfer systems is their size. The diffraction limit dictates that the smallest diameter within which power can be focused is proportional to the distance from the source and inversely proportional to the source's diameter. The Airy disk radius equation [23] illustrates this relationship for a uniformly illuminated transmitting circular aperture of radius a (radius is used here rather than diameter as is typical). At a distance R from a source transmitting at wavelength λ, the main beam's radius (measured at the first null) is given by

$$r_0 = \frac{0.61\lambda R}{a} \tag{1}$$

[1]While atmospheric attenuation is very low at microwave frequencies, the effect of the atmosphere is further minimized since the beam travels *vertically* through the atmosphere. The atmosphere's exponential density profile ensures that the average atmospheric attenuation along the beam's path is much lower than if power was transferred between two points on the Earth's surface.

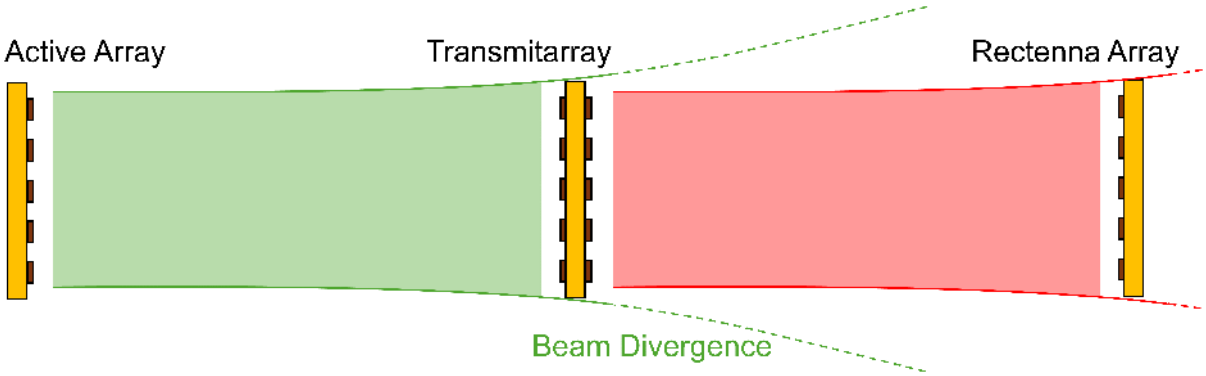

FIGURE 1. Transmitarray wireless power transfer system. The transmitarray refocuses the divergent beam from the transmitter, extending its range.

The radially integrated power from 0 to r_0 is roughly 84% of the total power in the pattern. Accordingly, to capture 84% of the transmitted power, the transmitter or receiver must scale at least linearly with the distance [3], [20]. For example, a transmitter operating at 10 GHz in geostationary orbit (GEO) ($\sim$36,000 km above the Earth's surface) requires a 1.6 km diameter to focus its main beam onto a 1 km diameter receiving station on Earth [3], [22].

This scaling challenge is further exacerbated by the number of array elements in a phased array of this size. Phased arrays' efficient spatial power combining and ability to create dynamic focal points using electronic steering makes them an ideal choice for wireless power transmitters [3], [24], [25], [26]. However, they require dense element spacing ($\sim$ $\lambda/2$) to avoid grating lobes (the so-called "sparse array curse"), leading to extremely large element counts. Avoiding grating lobes is especially important for wireless power transfer since they lead to major efficiency reductions.

Furthermore, elements must be synchronized to the same frequency source and their relative phases must be maintained over all operating conditions. Complex distribution networks are required to provide a phase-stable, low phase-noise frequency reference to elements in such arrays. This challenge also exists for retroreflective arrays where an absolute phase reference is assumed (sometimes implicitly) in order to perform the necessary phase conjugation.[2] Work has been done to address challenges associated with large-scale synchronization of phased arrays beyond typical RF distribution networks. These include optical distribution techniques for low loss distribution over long distances [27] and wireless techniques for distributed array synchronization and timing alignment [28]. Still, the prospect of synchronizing large numbers of elements, potentially billions of elements in the case of space solar power [22], is daunting.

One way to address this challenge is to refocus the power from the transmitter (hereafter called the active array) on its way to the receiver using a transmitarray, working as a passive relay, as shown in Fig. 1. The active array is focused to a transmitarray, which acts as a microwave lens [29], reshaping the wavefront and refocusing the beam to the receiver (or to yet another transmitarray to form a multi-stage relay chain). Since the transmitarray refocuses the active array's beam, the active array can be made significantly smaller without increasing the rectenna array's size. This is desirable for two reasons. First, unlike the active array, the transmitarray requires no synchronization since the incident wavefront is the transmitarray's reference. Second, the transmitarray is significantly cheaper than the active array, lacking much of the latter's active components and complexity. Note that the transmitarray is a passive relay; it does not introduce new energy to the beam nor does it modify the beam's frequency. The only electronic components required for the transmitarray are electronically tunable phase shifters and basic digital control.

In this work, we propose a space solar power concept at 10 GHz consisting of a multi-orbit constellation of phased arrays in geostationary orbit (GEO) and transmitarrays in medium Earth orbit (MEO). 10 GHz is chosen following the trend of recent wireless power transfer research conducted at X-band [2], [3], [7], [19], [22], [24], [30]. Using physical optics and the technoeconomic analysis in [22], a cost model of the system is developed. It is shown that using transmitarrays for space solar power can reduce the system's LCOE considerably for certain active array diameters.

The remainder of the paper is organized as follows: Section II discusses hardware-related challenges and solutions for transmitarrays in space; Section III introduces our cost model based on the results in [22] and the methods used to accurately simulate the proposed system, and discusses a key scnario in which transmitarrays significantly lower the system's LCOE; Section IV presents a static transmitarray hardware prototype and measurements illustrating its ability to refocus power in the context of wireless power transfer; finally, Section V presents our conclusions.

II. HARDWARE SOLUTIONS

For a space-based solar power system, the system efficiency and cost, and the space solar power station's physical flexibility and areal mass are driving factors that determine the system's practicality. Numerous solutions that minimize areal

[2]In fact, it may even be more challenging in retroreflective arrays where an absolute reference is needed instead of a stable yet arbitrary phase reference as used in [3].

mass and cost while maximizing efficiency and flexibility of different system components have been explored [7], [8], [24], [25], [30], [31], [32], [33]. While most of this research pertains to active phased arrays, many of the techniques carry over to transmitarrays due to the similarities between them.

The layered approach for phased arrays explored in [24], [25] is one method that satisfies the stringent requirements on flexibility and areal mass. However, to increase flexibility and mechanical robustness, we restrict our design space to layered designs without inter-layer electrical connections, relying instead on electromagnetic coupling between the layers. We consider two possible design approaches that are amenable to our goals: the frequency selective surface approach and the receiver-transmitter approach. We show that the latter is preferable for our unique application.

A. MULTI-LAYER FREQUENCY SELECTIVE SURFACE APPROACH

A ML-FSS consists of N, arbitrarily patterned, conducting layers separated by substrates. The airgap substrate is well-suited for the large, flexible, collapsible structures we are interested in.[3] Unfortunately, as discussed in [34], ML-FSS's involve an inherent trade-off between the number of layers, the transmission loss, and the transmission phase shift range. This trade-off appears most clearly in a transmission line model where each layer in the ML-FSS is represented by a single reactive shunt discontinuity with the ABCD parameter matrix [35],

$$A = \begin{pmatrix} 1 & 0 \\ jB & 1 \end{pmatrix}. \tag{2}$$

where B is the susceptance of the shunt impedance.

Computing the magnitude and phase of the S-parameters, we find that the two components are not independent but are related by

$$|S_{21}| = \cos \angle S_{21}. \tag{3}$$

Changing the transmission phase necessarily results in a change in the transmission magnitude. This means that for a given amount of loss, there is an upper bound on the achievable phase range. E.g., if we require $|S_{21}|^2 > 0.9$ (<1dB loss), only 52 degrees of phase range can be achieved, a far cry from the desired 360 degrees.

Reference [34] empirically extends this result for 2, 3 and 4 layer ML-FSS designs with *identical* layers. In particular, they demonstrate that a 4 layer ML-FSS is required to achieve 360 degrees of transmission phase range with less than 1dB of loss. Importantly, if non-identical layers are permitted, 360 degrees phase range can be obtained with 3 layers. However, such a design requires individual, independent control of all three layers, substantially increasing the digital routing requirements.

[3]We are specifically referring to the lack of *electronic* layer interconnects. Of course, the final design will need mechanical interconnects to maintain the separation between the layers, whether those be the carbon fiber S-springs used in [25], a foam substrate, or something else.

TABLE 1. Physical Design Parameters for the 3-Layer Transmitarray Unit Cell Design Depicted in Fig. 2

Param.	Symbol	Value	Unit
Patch width	W_{patch}	14.00	mm
Patch length	L_{patch}	12.45	mm
Slot width	W_{slot}	9.00	mm
Slot length	L_{slot}	0.50	mm
Microstrip width	W_{feed}	127	μm
Copper thickness	t_{cop}	15.0	μm
Airgap thickness	h_{airgap}	1	mm
Substrate thickness	t_{sub}	25.4	μm
Unit cell period		0.6	λ

B. RECEIVER-TRANSMITTER APPROACH

The receiver-transmitter approach overcomes the limitations of the ML-FSS approach by breaking the assumption underpinning the transmission line model, i.e., that the incident wave remains in the TEM mode as it propogates through the transmitarray. This approach uses two back-to-back antennas coupled by a transmission line as in [36], [37], [38], [39]. For a static transmitarray where the phase shift gradient across the array is fixed, changing the transmission line length across the array introduces a phase gradient; for a reconfigurable transmitarray, programmable phase shifters are added along the transmission line. While in a ML-FSS, every layer contributes a pole to the transfer function, any number of poles can be introduced to a receiver-transmitter transmitarray along the transmission line using lumped elements and/or transmission line segments. With three mechanical layers (two antenna layers and one transmission line layer), an arbitrary phase shift range can be achieved, subject only to the losses in the transmission lines and phase shifter. These losses are not trivial, but are not fundamentally bounded as they are for a ML-FSS as illustrated by (3).

To validate our conclusion we design and simulate a static receiver-transmitter 3-layer transmitarray[4] unit cell, operating at 10 GHz. Since this design meets our unique set of requirements in that it is flexible, has no electrical interconnects between layers, and can achieve a loss below 1dB, it can serve as a starting point for designing wireless power transfer transmitarrays in the future.

The layers are as follows (see Fig. 2):

1) the receiving patch antenna
2) a transmission line and ground plane separated by a polyimide substrate
3) the transmitting patch antenna

The physical design parameters are listed in Table 1. Since the transmitting and receiving antennas share a ground plane, special care was taken to avoid direct coupling between the

[4]Here, we are referring to mechanical layers rather than conductor layers. Technically, four conductor layers are needed: two antenna layers, a transmission line layer and a ground plane. However, the transmission line and ground plane are fabricated on the same flexible PCB, effectively forming a single layer. In the ML-FSS approach, layers this close (25 μm) to each other would behave as a single layer due to very high capacitive coupling.

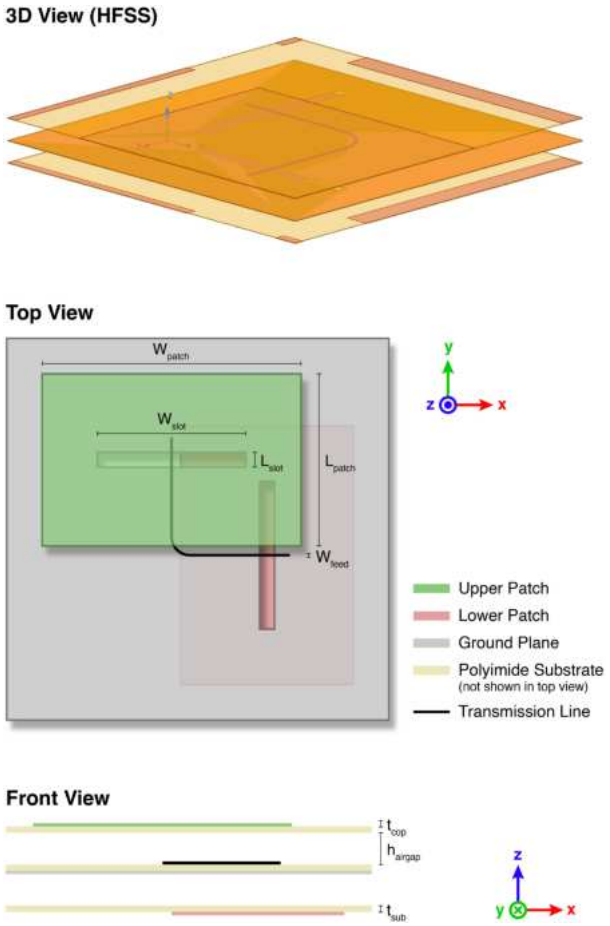

FIGURE 2. Diagram (3D screenshot, top, and front views) of the 3-layer transmitarray unit cell showing the physical elements of the design. The dimension labels correspond to those in Table 1.

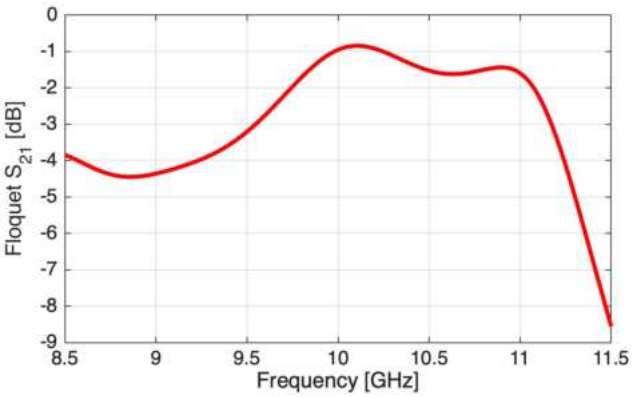

FIGURE 3. Simulated S21 for the transmitarray unit cell under normal incidence.

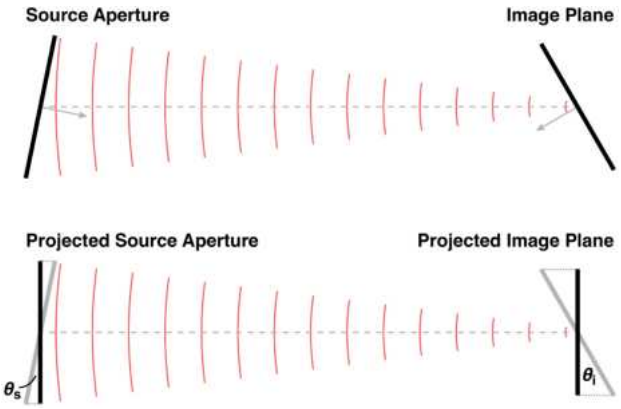

FIGURE 4. Geometry for our approximation permitting application of the Fresnel diffraction formula to large angles of diffraction.

transmitting and receiving antennas through the apertures in the ground plane. We accomplished this by rotating the two patch antennas and their corresponding slots by 90 ° relative to one another, ensuring that the polarizations of the two antennas are mutually incompatible. To demonstrate the feasibility of this design and a loss of less than 1dB, it was simulated in HFSS; the simulated S21 at normal incidence is shown in Fig. 3.

III. COST ANALYSIS

A. PHYSICAL OPTICS MODEL

While unit cell-based infinite-array simulations work well for designing the unit cells themselves, we seek another tool for modeling the effects of arrays with very large numbers of elements that are nonetheless finite in extent. Since the dimensions of the arrays in a space solar power system are much larger than the wavelength, physical optics is a suitable tool for their analysis. In particular, we use the Fresnel diffraction model since the transmitarray, active array and rectenna array are located in each other's radiative near field regions.

As shown in Fig. 4, we work with *projected* source and image planes that are both parallel to each other and orthogonal to the direction of propagation. This allows us to compute approximate diffraction patterns at large steering angles. It is important to note that for an arbitrary aperture to steer a *focused* beam to a particular point in space, it must introduce two phase gradients: a linear gradient steers the beam in a particular direction and a quadratic gradient focuses the beam at a given distance from the aperture.

To compute the pattern, we follow this simple process:

1) Replace the source aperture with its projection onto the projected aperture plane, i.e., shrink aperture by $\cos\theta_s$. Because the projected source is perpendicular to the direction of propagation, the linear phase gradient is removed from the phase distribution.
2) Compute the Fresnel diffraction pattern of the projected aperture
3) "Unproject" the source plane, i.e., stretch pattern by $1/\cos\theta_i$

The algorithm described above works when the relative rotation of the source and image planes are in the same axis. When the two planes do not share a rotation axis, the algorithm can easily be extended by shrinking/stretching the source/image planes along different axes.

TABLE 2. Unit-Area Cost of the Transmitarray (T.A.) Derived From the Active Array (A.A.) Costs Provided in [22]

	Unit	A.A.	Multiplier	T.A.
Initial Costs	**$/m^2**	**293**		**102**
PV	$/m^2	95	0	0
WPT	$/m^2	95	0.25	24
Structures	$/m^2	34	1	34
Spacecraft	$/m^2	28	1	28
Assembly	$/m^2	28	0.5	14
Testing	$/m^2	14	0.2	3
Mass	**kg/m^2**	**0.28**		**0.14**
PV	kg/m^2	0.090	0	0
WPT	kg/m^2	0.089	0.4	0.035
Structures	kg/m^2	0.032	1	0.032
Spacecraft	kg/m^2	0.073	1	0.073
Launch Costs	**$/m^2**	**36.4**		**12.0**
Cost/launch	$M	7.0	1	7.0
Mass/launch	kg	54500	1.5	81750
Upkeep Costs	**$/m^2**	**24.7**		**4.2**
Lifetime	yr	15	1	15
Failure rate	%/yr	0.5	0.5	0.25
Total Cost	$/m^2	**354**		**118**

To verify its validity, we tested this method and compared it against the Huygens-Fresnel principle. In particular, we compared the integrated power in a circular area as a function of the circle's radius. We found less than a 1% deviation even at large angles of diffraction ($\sim$ 50°). The radially integrated power metric is important for wireless power transfer since we are ultimately concerned in how much power is captured by a receiver of a given radius.

B. UNIT-AREA COST MODEL

Once the diffraction patterns are computed, we can determine the amount of power captured by a receiving aperture (whether that be the transmitarray or the rectenna array) as a function of that aperture's area. Since we ultimately want to minimize some cost function, we relate the area of each array to its total cost using a per-unit-area cost. For the active and rectenna arrays, we rely on the technoeconomic analysis presented in [22] (see Table 2, "middle" column) to calculate unit area costs for the active array and the rectenna array (ground station). The unit area costs are calculated by dividing the total cost of each array ($\mathrm{COST}_{\mathrm{total}} = \mathrm{COST}_{\mathrm{initial}} + 15 \cdot \mathrm{COST}_{\mathrm{annual}}$) by the area of each array. For the active array we obtain $c_{\mathrm{tx}} = 354$ \$/m^2, and for rectenna array, $c_{\mathrm{rx}} = 121$ \$/m^2. These values naturally assume that all costs scale linearly with area which is approximately true as long as none of the arrays become too large or too small.

Because transmitarrays are not part of [22], we use the active array cost breakdown as the basis for our transmitarray cost model due to the many similarities between the transmitarray and active array hardware. In Table 2 we break down the transmitarray costs into initial, launch, and annual upkeep costs (transmitarray module replacement) and show how they are derived from the active array cost model. The reduction in WPT costs and mass is due to a lack of RF integrated circuits, pop-up antennas and heavy DC transmission lines. Assembly, testing costs and failure rate are also reduced since the transmitarray is significantly less complex than the active array. Finally, mass per launch increases because the transmitarrays are located in MEO instead of GEO.

One part of the transmitarray that will be more expensive than the active array will be radiation shielding due to the higher radiation effects in MEO versus in GEO. However, because the vast majority of the transmitarray is passive, the additional shielding that will be required for the electronics is small.

C. TRANSMITARRAY CONSTELLATION

In a system composed of one active array, one transmit array and one rectenna array, the system will only be able to operate as intended for a small portion of the transmitarray's orbit. As the transmitarray orbits the Earth, it will periodically approach the line-of-sight path between the active and rectenna arrays, cross that path, and then move away, eventually being eclipsed by the Earth. For the small orbital segment where the transmitarray is more or less aligned with the other two arrays, transmission through the transmitarray can occur as intended (see Fig. 5(a)). Otherwise, both the arrival/departure angles at the transmitarray and the additional distance traveled between the arrays will lead to energy losses that make the transmitarray virtually useless (see Fig. 5(b)).

To avoid this energy loss, we propose a constellation of N_{ta} equally-spaced transmitarrays occupying the same orbit. As one transmitarray moves away from the active array, another transmitarray will approach so that when the first moves out of range, the active array will quickly refocus its beam to the next transmitarray (see Fig. 5(c)). While this will increase the system's total cost, it will decrease its LCOE. For example, if a single transmitarray can only be used for 1/5 of its orbit, using a transmitarray constellation of 5 will increase the energy beamed to Earth by a factor of 5. Meanwhile, the system's total cost increases by a factor much less than 5.

We also propose increasing the number of active and rectenna arrays to match the number of transmitarrays (see Fig. 6). If only one active array and rectenna array are used, only one transmitarray will ever be in use at a given time, leading to significant overhead. This overhead can be eliminated by matching each unused transmitarray with its own active array and rectenna array (of course, the specifc transmitarray used by a given active array will change as the transmitarrays orbit). This triple constellation will decrease the LCOE even further: a constellation of 10 active arrays and rectenna arrays used along with 10 transmitarrays increases the total energy output of the system by 10 relative to a system with 10 transmitarrays but only one active and rectenna array. However, the total cost of the system clearly increases by less than a factor of 10 meaning LCOE must decrease.

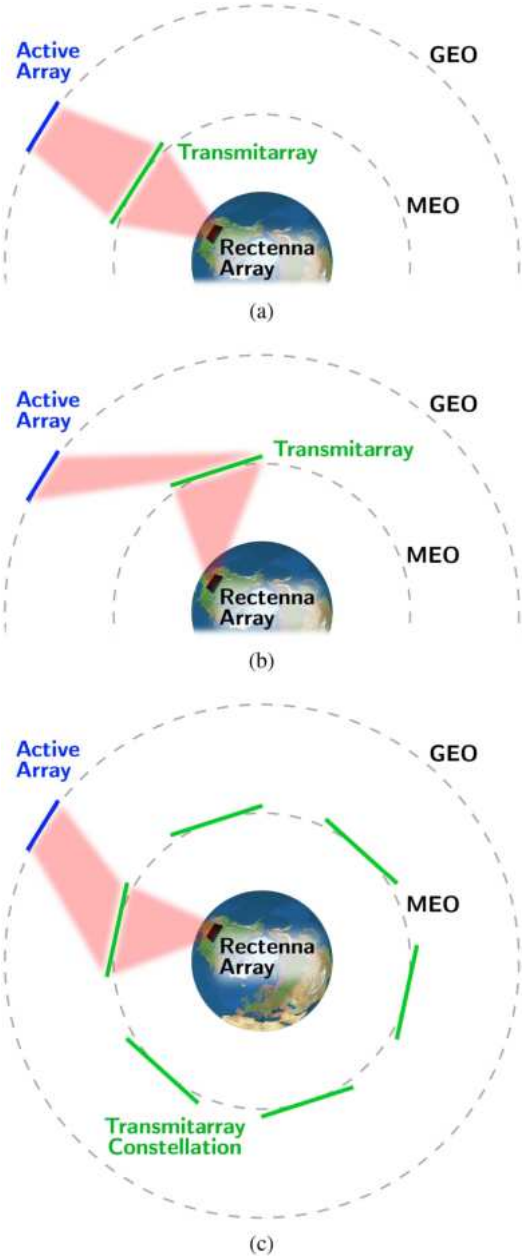

FIGURE 5. Cartoon showing (a) power transfer when transmitarray is aligned with direction of power transfer, (b) power transfer when transmitarray is not well-aligned with the direction of power transfer, and (c) power transfer with a transmitarray constellation–the active array can now beam through a transmitarray that is both closer and better aligned with the direction of power transfer.

A full constellation is shown in Fig. 6 where there are 6 of each array. Each active array will always steer to follow the closest transmitarray. As the transmitarrays orbit the Earth, the active arrays will periodically refocus their beams to the next transmitarray.

D. RESULTS

As developed in [22], the system's LCOE and the system's total cost are two possible cost functions. When transmitarrays are used, the system's total cost is always greater

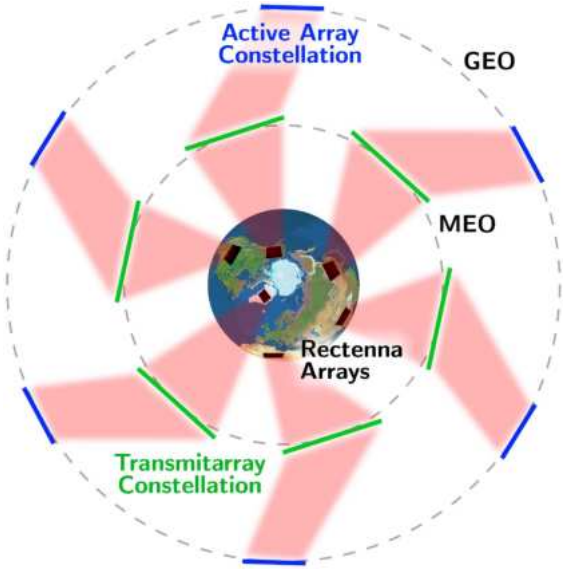

FIGURE 6. Cartoon showing a full constellation including active arrays, transmitarrays, and rectenna arrays. As the transmitarrays move through their orbits, the active arrays continuously adjust their beams to focus on the nearest transmitarray.

due to the need of a constellation as discussed in the preceding section. On the other hand, adding a transmitarray constellation *can* reduce the LCOE. Of course, if only LCOE is considered, the largest possible active array should be used. Clearly this is impractical since there will be some maximum active array size that will be practical, likely due to synchronization challenges. Since research on synchronization schemes for large-scale arrays is ongoing, we leave the active array size as the independent variable in our analysis. For each active array size, we compute the system's cost with and without transmitarrays to determine whether, for that particular active array, transmitarrays are advantageous.

The program used to compute the LCOE takes the following parameters:

- Size of the active array: independent variable
- Desired capture efficiency of the transmitarray: $\eta_{TA,cap} = 0.7$ (The capture efficiency specifies the percentage of the active array's radiated power that is incident upon and captured by the transmitarray.)
- The transmitarray's internal efficiency (includes losses in phase shifters and antennas): $\eta_{TA} = 0.9$
- # of active arrays/transmitarrays/rectenna arrays in the constellation: $N = 10$
- Operating frequency: 10 GHz
- Array Orbits/Locations: Active array is in GEO, rectenna array is directly below the active array, transmitarrays are in MEO with an altitude half that of GEO
- Array Orientations: Active array and transmitarrays are pointed at nadir
- The number of points in the transmitarray's discretized orbit

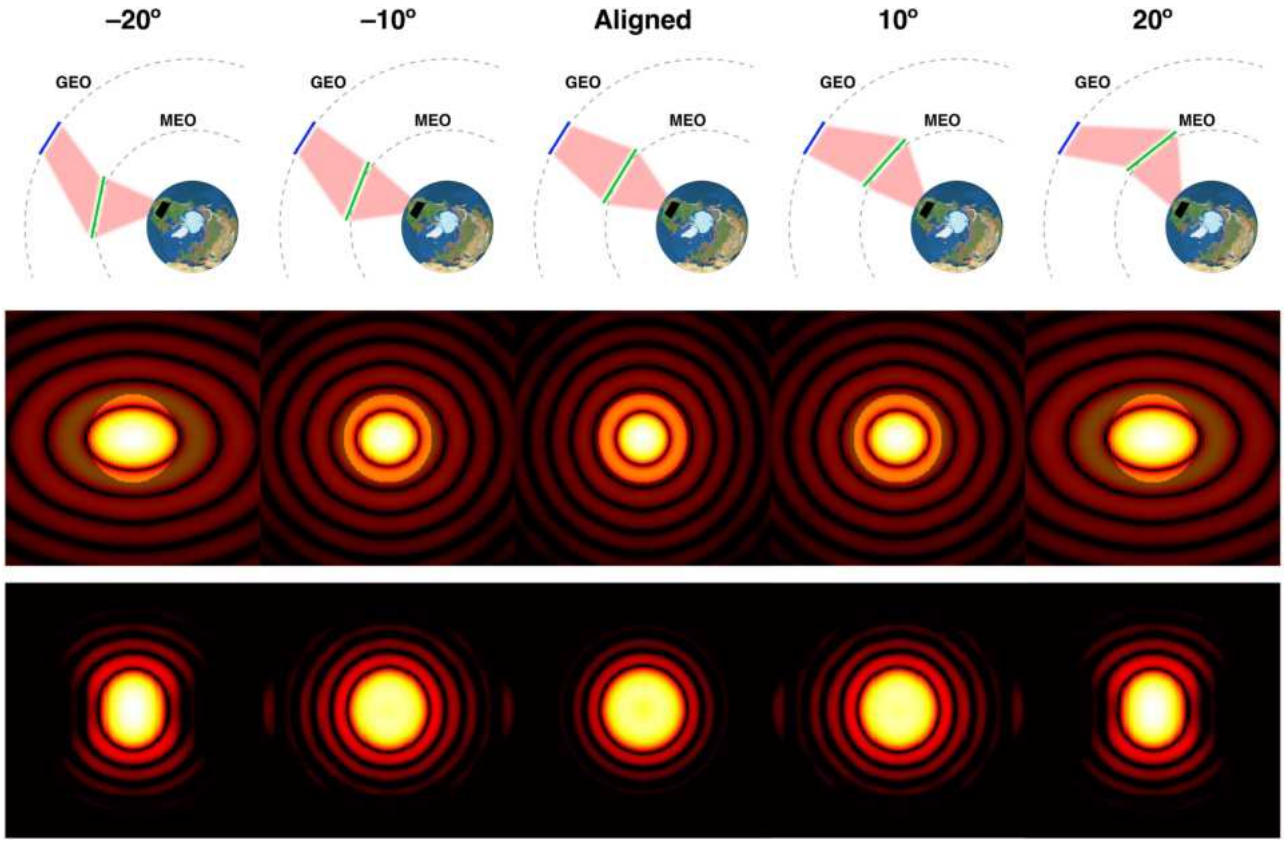

FIGURE 7. Diffraction patterns of the active array at the transmitarray plane (middle) and of the transmitarray at the rectenna plane (bottom) for five points as the transmitarray moves through its orbit (top). The part of the active array's pattern that falls outside the transmitarray is greyed out; The power in the circle is reradiated by the transmitarray towards the rectenna array. In this case, $N = 9$ so that each transmitarray has an effective orbital span of 40 °.

- The efficiency of the system due to factors other than non-unity capture efficiencies. This includes photovoltaic losses, DC to RF conversion loss, rectenna losses, etc.: 6%(see [22])[5]

We neglect the effects of polarization mismatch and additional losses at large steering angles. The latter can be due to antenna element patterns and impedance mismatch resulting from mutual coupling changes. These factors have the potential to increase losses beyond what is considered here but can be mitigated. Polarization mismatch is typically mitigated by using circular polarization. Issues at large scan angles can be reduced by restricting the maximum scan angle; in this system, that is accomplished by using a larger constellation.

Given the parameters above, the program computes the minimum achievable LCOE. The program chooses the minimum LCOE because the rectenna array size is not fixed; for every rectenna size there is a different LCOE. The transmitarray size, however, is indirectly fixed by specifying η_{TA}. A summary of the algorithm is below.

1) The effective transmit array orbital span is calculated as $360^\circ/N$. The orbital span is the part of the transmitarray's orbit actually used for computation since the diffraction patterns are periodic.
2) The active array's focused and steered diffraction pattern is computed at the transmitarray's location for each point in the transmitarray's orbital span (see Fig. 7 middle row).
3) The transmitarray's captured power as a function of its diameter is computed from the diffraction pattern.
4) The size of the transmitarray is determined to meet the specified capture efficiency parameter.
5) The transmitarray's focused and steered diffraction pattern is computed at the rectenna array's location for each point in the transmitarray's orbital span (see Fig. 7 bottom row).
6) The rectenna array's captured power as a function of its diameter is computed from the diffraction patterns and, from that, the LCOE as a function of the diameter.
7) Finally, the rectenna array size is chosen to minimize LCOE.

This process is repeated for each active array diameter.

A critical part of this process is computing the diffraction pattern of the active array on the transmitarray, and of the

[5] 6% is based on the middle column in [22] Table 1 with η_{ground} and η_{geom} excluded.

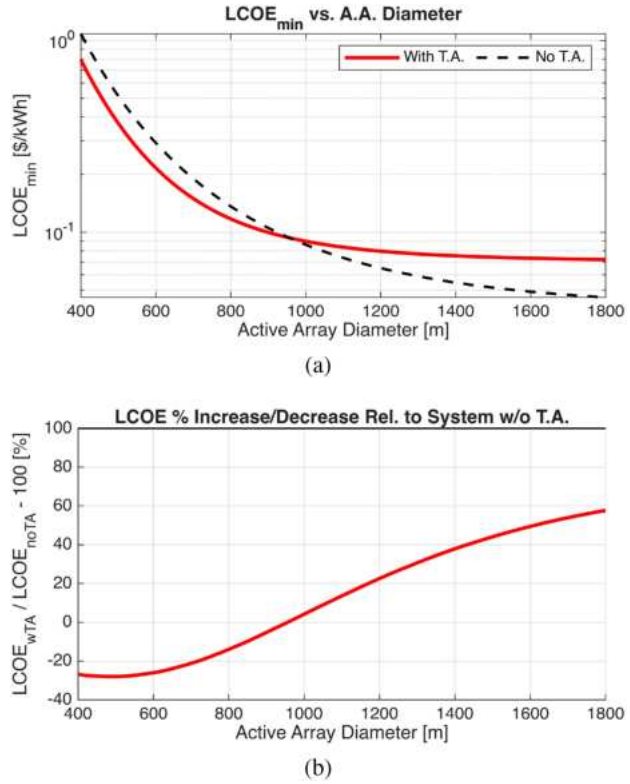

FIGURE 8. Cost analysis results. A.A. = active array. T.A. = transmitarray. For each active array diameter we plot (a) the minimum achievable LCOE both with and without transmitarrays and (b) LCOE percent increase/decrease relative to the LCOE without transmitarrays.

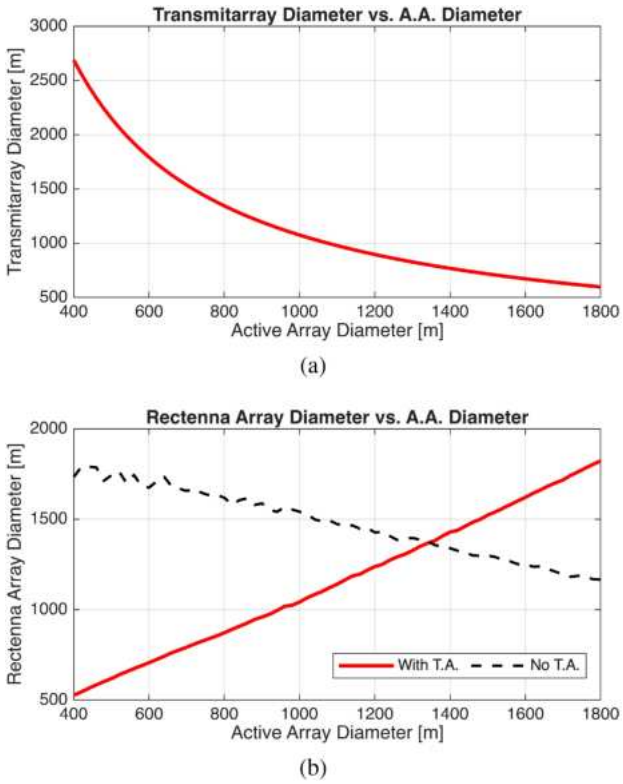

FIGURE 9. The transmitarray (a) and rectenna array (b) diameters for which the minimum LCOE in Fig. 8(a).

transmitarray on the rectenna array. Exemplary patterns are shown in Fig. 7. We assume that the active arrays, transmitarrays and rectenna arrays are periodically spaced around Earth. While the rectennas will not necessarily be periodic, making this assumption significantly reduces computation time since the periodicity of each array type means the patterns themselves are periodic as the transmitarray moves through its orbit. The patterns need only be computed for one active array/transmitarray/rectenna array set and only for the part of the transmitarray's orbit where it is closest to the active array, i.e., the effective orbital span $360^\circ/N$.

In Fig. 8(a), we show the minimum LCOE, LCOE $_{\text{min}}$, that can be achieved by the 3-tier constellation. We also plot the minimum LCOE that can be achieved in a system of just one active array and rectenna array but no transmitarray (dashed black line). The percent increase/decrease in the LCOE compared to the system without transmitarrays is shown in Fig. 8(b)). This is a critical comparison because it tells us which systems (in terms of active array diameters) benefit from using a transmitarray. We conclude that introducing transmitarrays to the system lowers the LCOE for active array diameters below roughly ~ 1000 m for this particular set of parameters.

Intuitively, this is motivated by the inverse scaling of a diffraction pattern relative to the size of its source. Since the active array illuminates the transmitarray, the transmitarray diameter is inversely proportional to the active array diameter to the first order (see Fig. 9(a)). Similarly, the rectenna array scales inversely with the transmitarray and so it must scale directly with the active array (see Fig. 9(b)). If the active array is made very large, then the transmitarray will become very small requiring the use of a very large rectenna array. At some point, the transmitarray will be small enough that it would be better to just beam directly to earth.

An important side-effect of this analysis is that systems where a transmitarray is advantageous will have very small spot-sizes on the ground, as shown in Fig. 9(b). This can be extremely valuable for locations where land is available at a premium. A small rectenna array would also be useful for military applications and natural disaster relief. Small, temporary rectenna arrays could be constructed very quickly and torn down equally fast when no longer needed.

The downsides of using transmitarray systems are twofold. First, the transmitarray's size effectively substitutes for the active array's size. Thus, the transmitarray sizes are extremely large, on the order of 1–3 km in diameter as shown in Fig. 9(a). However, we note that constructing a transmitarray of this size is much more feasible than constructing a similarly sized

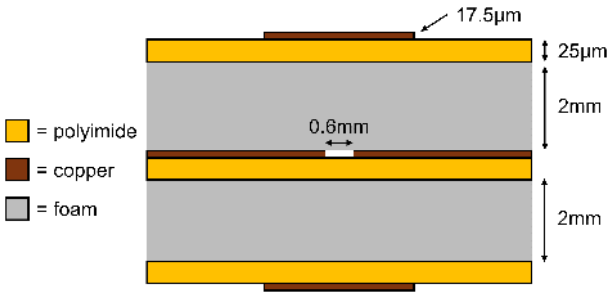

FIGURE 10. Transmitarray prototype stack-up. The outer layers are patch antennas with a slot in the middle for coupling.

active array since a synchronization scheme is not required. Second, to achieve the LCOE's presented in Fig. 8(a), the system requires a constellation of 10 arrays at each level. As the constellation size grows beyond 10, the gap between the two curves in Fig. 8(a) grows, but only to a point. If the constellation size is reduced sufficiently, the gap will close and there will not be any point where transmitarrays are beneficial. This is indicative of a trade-off between total system cost and complexity, and the system's LCOE.

IV. TRANSMIT-ARRAY PROTOTYPE

An important assumption underlying the cost analysis presented above is that transmitarrays can be made cheaply and with very low areal mass. To demonstrate the feasibility of a lightweight and affordable transmitarray, we fabricated a static transmitarray using a low-cost, standard, commercial flexible PCB process and low-cost off-the-shelf materials. The design of this prototype relies on the more common ML-FSS approach for transmitarray design since the purpose of this prototype is to illustrate the feasibility of this PCB process rather than create a very low-loss transmitarray.

Each layer consists of a flexible single-layer PCB each constructed on a 25 μm thick polyimide substrate with 1/2 oz. copper. A gap of 2 mm is maintained between each of the layers using low-cost EVA foam with a measured dielectric constant of 1.12 and negligible loss. Electromagnetically, the transmitarray is a 16×16 $\lambda/2$ unit cell grid where each cell consists of two identical patch antennas (the outer two layers) coupled through a slot (Fig. 10) [40], [41]. The phase gradient was introduced by varying the slot length between 4 mm and 9 mm across the transmitarray. A photo of the fabricated prototype is shown in Fig. 11.

To measure transmitarray's focusing capability, we illuminated it with 256-element phased array located 2.5 m directly behind the transmitarray. At a distance of 1.3 m on the other side of the transmitarray, a near field scanner was used to measure the power distribution across a roughly 1m× 1 m square both with and without the transmitarray in place (Fig. 13). The measurement setup is shown in Fig. 12. The

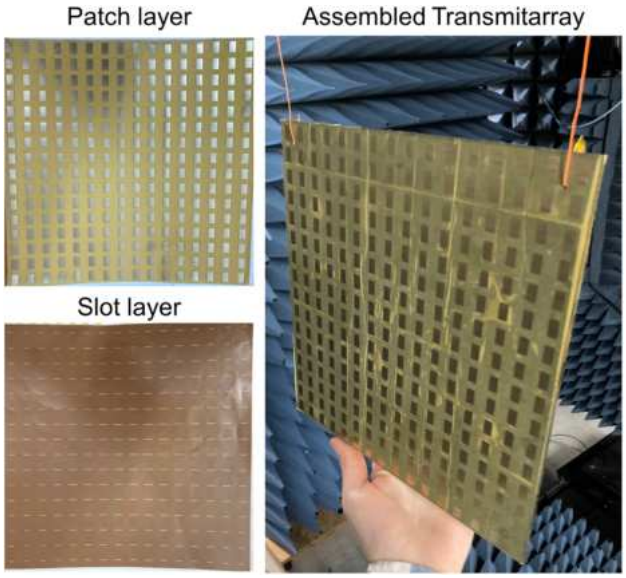

FIGURE 11. Fabricated transmitarray prototype: individual layers (left) and assembled array (right).

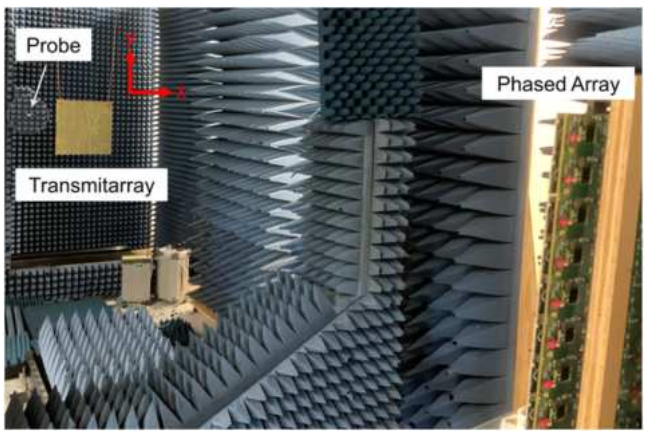

FIGURE 12. Prototype transmitarray measurement setup.

transmitarray increases the peak power density by 3.5dB compared to the phased array by itself, and reduces the -3dB beam area by approximately 75%.

To demonstrate the transmitarray's ability to boost power delivered to a rectenna array receiver, a 5×5, 0.5λ pitch (7.5 cm× 7.5 cm) rectenna array [7] was placed at the center of the main-beam using the probe scanner. The phased array was focused to the rectenna using using a closed-loop feedback algorithm to maximize power transmission [30]; a plot of the voltage at the rectenna while focusing is shown in Fig. 14. The peak rectified voltage, V_r, which feeds into a 54 Ω load, increases by a factor of 1.54, corresponding to a 2.37x increase in the rectified power, P_r.

A summary of the rectifier measurements are provided in Table 3. Because the efficiency of the rectenna, η_{RF-DC},

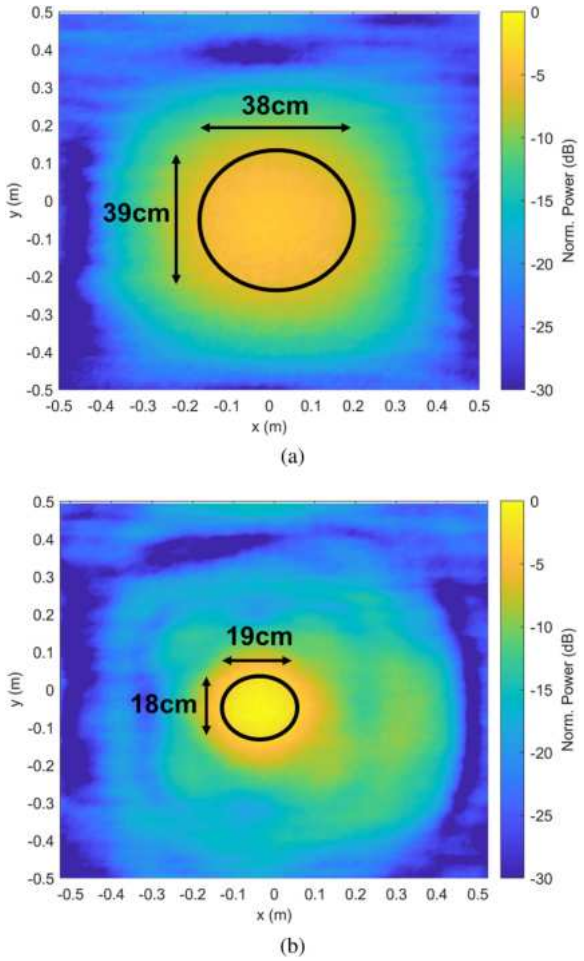

FIGURE 13. Normalized power densities (a) without the transmitarray and (b) with the transmitarray. Intensity values are normalized to the maximum intensity measured *with* the transmitarray. Black ellipses correspond to the -3db contours of each plots respective peak.

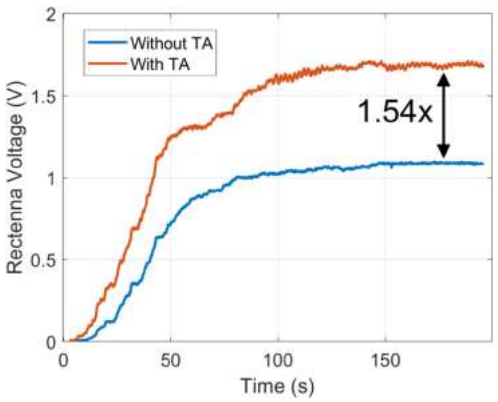

FIGURE 14. Rectenna output voltage while focusing. The rectenna DC output is terminated by a 54 Ω load in both cases.

TABLE 3. Rectenna Focusing Experiment Results

	P_i	V_r	P_r	η_{RF-DC}
No TA	44 mW	1.1 V	22 mW	50%
TA	78 mW	1.7 V	54 mW	69%

changes as a function of the incident power, P_i, more information is required in order to state that an increase in P_r implies an increase in P_i. By integrating the power measurements in Fig. 13 over the rectenna area, we find that P_i increases by a factor of 1.77 when the rectenna is added, confirming that the transmitarray *does* increase the power density at the rectenna. Consequently, the 2.37x increase in P_r is due in part to the efficiency improving from 50% to 69% [7] and in part due to the transmitarray's focusing.

V. CONCLUSIONS AND FUTURE WORK

Above we have provided a theoretical discussion of transmitarrays in the context of wireless power transfer and, specifically, space solar power. We provide initial work on transmitarray unit cell designs that enable a large range of transmission phase settings while maintaining low loss, the paramount concern in any wireless power transfer system. At the system level, the cost analysis shows that transmitarrays can increase the feasibility of space solar power by lowering the system's LCOE, thus lowering the cost of power delivered to consumers. In terms of flexibility, transmitarrays also reduce the size of the rectenna array on the ground, increasing the system's potential for emergency and military applications where quick access to electricity is essential. Finally, we conclude with a practical demonstration showing that low-cost, low-mass transmitarrays can significantly increase the amount of power transferred in a wireless power transfer system.

Future work on transmitarrays in the context of wireless power transfer may include fabrication of the design discussed in Section II along with alternative designs. With respect to the cost analysis, one important variable neglected in this paper was the operating frequency. As shown by the frequency analysis in [22], the calculus for the optimal frequency can change significantly depending on the cost function. We expect that doing a cost study that includes frequency will show that further LCOE reductions are possible at other frequencies given diffraction's λ-dependence.

However, even considering only a single frequency, we believe that our results demonstrate that transmitarrays can play an important role in the implementation of a economically viable space solar power system. More importantly, they may prove key to enabling space solar power from a technological perspective by decreasing the synchronization requirements, one of the most significant challenges facing space solar power today. The work presented in this paper can serve as a starting point for fruitful discussion, research, and development leading us closer to a vision of clean solar power delivered from space.

REFERENCES

[1] C. T. Rodenbeck et al., "Terrestrial microwave power beaming," *IEEE J. Microwaves*, vol. 2, no. 1, pp. 28–43, Jan. 2022.

[2] C. T. Rodenbeck et al., "Microwave and millimeter wave power beaming," *IEEE J. Microwaves*, vol. 1, no. 1, pp. 229–259, Jan. 2021.
[3] A. Hajimiri, B. Abiri, F. Bohn, M. Gal-Katziri, and M. H. Manohara, "Dynamic focusing of large arrays for wireless power transfer and beyond," *IEEE J. Solid-State Circuits*, vol. 56, no. 7, pp. 2077–2101, Jul. 2021.
[4] N. Shinohara, "History and innovation of wireless power transfer via microwaves," *IEEE J. Microwaves*, vol. 1, no. 1, pp. 218–228, Jan. 2021.
[5] W. C. Brown, "Experimental airborne microwave supported platform," Raytheon Co Burlington, MA Microwave and Power Tube Div, 1965.
[6] R. Dickinson, "Evaluation of a microwave high-power reception-conversion array for wireless power transmission," Jet Propulsion Laboratories, Tech. Rep. JPL-TM-33-741, 1975.
[7] A. Ayling et al., "Wireless power transfer in space using flexible, lightweight, coherent arrays," 2024. [Online]. Available: https://arxiv.org/abs/2401.15267
[8] A. Ayling et al., "Wireless power transfer in space using flexible, lightweight, coherent arrays," *Acta Astronautica*, vol. 224, pp. 226–243, 2024. [Online]. Available: https://www.sciencedirect.com/science/article/pii/S009457652400434X
[9] P. E. Glaser, "Power from the Sun: Its future," *Science*, vol. 162, no. 3856, pp. 857–861, 1968. [Online]. Available: https://www.science.org/doi/abs/10.1126/science.162.3856.857
[10] W. C. Brown, "Satellite power stations: A new source of energy?," *IEEE Spectr.*, vol. MSPEC-10, no. 3, pp. 38–47, Mar. 1973.
[11] DOE/NASA, "DOE/NASA satellite power system concept development and evaluation program, satellite power system (SPS) FY79 program summary," DOE/ER-0037, Washington, DC, USA, 1980.
[12] J. C. Mankins, "A technical overview of the 'suntower' solar power satellite concept," *Acta Astronautica*, vol. 50, no. 6, pp. 369–377, 2002. [Online]. Available: https://www.sciencedirect.com/science/article/pii/S0094576501001679
[13] W. Seboldt, M. Klimke, M. Leipold, and N. Hanowski, "European sail tower SPS concept," *Acta Astronautica*, vol. 48, no. 5, pp. 785–792, 2001. [Online]. Available: https://www.sciencedirect.com/science/article/pii/S0094576501000467
[14] M. Mori, H. Kagawa, and Y. Saito, "Summary of studies on space solar power systems of Japan Aerospace Exploration Agency (JAXA)," *Acta Astronautica*, vol. 59, no. 1, pp. 132–138, 2006, Space for Inspiration of Humankind, Selected Proceedings of the 56th International Astronautical Federation Congress, Fukuoka, Japan, Oct. 17–21 2005. [Online]. Available: https://www.sciencedirect.com/science/article/pii/S0094576506001032
[15] S. Sasaki et al., "A new concept of solar power satellite: Tethered-SPS," *Acta Astronautica*, vol. 60, no. 3, pp. 153–165, 2007. [Online]. Available: https://www.sciencedirect.com/science/article/pii/S0094576506002815
[16] I. Cash, "CASSIOPeiA–A new paradigm for space solar power," *Acta Astronautica*, vol. 159, pp. 170–178, 2019. [Online]. Available: https://www.sciencedirect.com/science/article/pii/S0094576518320708
[17] Y. Yang, Y. Zhang, B. Duan, D. Wang, and X. Li, "A novel design project for space solar power station (ssps-omega)," *Acta Astronautica*, vol. 121, pp. 51–58, 2016. [Online]. Available: https://www.sciencedirect.com/science/article/pii/S0094576515300680
[18] X. Li, B. Duan, L. Song, Y. Yang, Y. Zhang, and D. Wang, "A new concept of space solar power satellite," *Acta Astronautica*, vol. 136, pp. 182–189, 2017. [Online]. Available: https://www.sciencedirect.com/science/article/pii/S0094576516311092
[19] B. Abiri et al., "A lightweight space-based solar power generation and transmission satellite," Accessed: Sep. 20, 2024. https://arxiv.org/abs/2206.08373
[20] P. Jaffe and J. McSpadden, "Energy conversion and transmission modules for space solar power," *Proc. IEEE*, vol. 101, no. 6, pp. 1424–1437, Jun. 2013.
[21] I. Asimov, *Reason*. New York, NY, USA: Street & Smith, Apr. 1941.
[22] O. Mizrahi et al., "Space solar power generation: A viable system proposal and technoeconomic analysis," *Res. Square*, Aug. 2024. doi: 10.21203/rs.3.rs-4747187/v1.
[23] J. Goodman, *Introduction to Fourier Optics*, 3rd ed. Englewood, CO, USA: Roberts and Company, 2005.
[24] M. Gal-Katziri, A. Fikes, F. Bohn, B. Abiri, M. R. Hashemi, and A. Hajimiri, "Scalable, deployable, flexible phased array sheets," in *Proc. IEEE/MTT-S Int. Microw. Symp.*, 2020, pp. 1085–1088.
[25] M. R. M. Hashemi et al., "A flexible phased array system with low areal mass density," *Nature Electron.*, vol. 2, no. 5, pp. 195–205, 2019.
[26] M. Gal-Katziri, A. Fikes, and A. Hajimiri, "Flexible active antenna arrays," *NPJ Flexible Electron.*, vol. 6, no. 1, 2022, Paper 85.
[27] M. Gal-Katziri, C. Ives, A. Khakpour, and A. Hajimiri, "Optically synchronized phased arrays in CMOS," *IEEE J. Solid-State Circuits*, vol. 57, no. 6, pp. 1578–1593, Jun. 2022.
[28] J. M. Merlo, S. R. Mghabghab, and J. A. Nanzer, "Wireless picosecond time synchronization for distributed antenna arrays," *IEEE Trans. Microw. Theory Techn.*, vol. 71, no. 4, pp. 1720–1731, Apr. 2023.
[29] Z. N. Chen et al., "Microwave metalens antennas," *Proc. IEEE*, vol. 111, no. 8, pp. 978–1010, Aug. 2023.
[30] F. Bohn, B. Abiri, and A. Hajimiri, "Fully integrated CMOS X-band power amplifier quad with current reuse and dynamic digital feedback (DDF) capabilities," in *Proc. IEEE Radio Freq. Integr. Circuits Symp.*, 2017, pp. 208–211.
[31] O. S. Mizrahi, A. Fikes, A. Truong, F. Wiesemüller, S. Pellegrino, and A. Hajimiri, "Popup arrays for large space-borne apertures," 2023. [Online]. Available: https://arxiv.org/abs/2308.07458
[32] O. S. Mizrahi, A. Fikes, A. Truong, F. Wiesemüller, S. Pellegrino, and A. Hajimiri, "Popup arrays for large space-borne apertures," *IEEE Trans. Antennas Propag.*, vol. 72, no. 8, pp. 6387–6400, Aug. 2024.
[33] A. C. Fikes, M. Gal-Katziri, O. S. Mizrahi, D. E. Williams, and A. Hajimiri, "Frontiers in flexible and shape-changing arrays," *IEEE J. Microwaves*, vol. 3, no. 1, pp. 349–367, Jan. 2023.
[34] A. H. Abdelrahman, A. Z. Elsherbeni, and F. Yang, "Transmission phase limit of multilayer frequency-selective surfaces for transmitarray designs," *IEEE Trans. Antennas Propag.*, vol. 62, no. 2, pp. 690–697, Feb. 2014. [Online]. Available: https://ieeexplore.ieee.org/document/6656844
[35] D. M. Pozar, *Microwave Engineering: Theory and Techniques*. Hoboken, NJ, USA: Wiley, 2021.
[36] T.-J. Li, G.-M. Wang, H.-P. Li, and H.-S. Hou, "Circularly polarized double-folded transmitarray antenna based on receiver-transmitter metasurface," *IEEE Trans. Antennas Propag.*, vol. 70, no. 11, pp. 11161–11166, Nov. 2022.
[37] Z. J. Zhai, F. Lin, G. Q. Zhao, and H. J. Sun, "A wideband thin transmitarray antenna by using l-probe patch antenna with true-time delay," *IEEE Antennas Wireless Propag. Lett.*, vol. 22, no. 10, pp. 2492–2496, Oct. 2023.
[38] L. Chang, Z. Zhang, and Z. Feng, "A three-layer transmitarray element with 360° phase range," in *Proc. IEEE Int. Symp. Antennas Propag. USNC/URSI Nat. Radio Sci. Meeting*, 2015, pp. 1868–1869.
[39] P. Padilla, A. Muñoz-Acevedo, M. Sierra-Castañer, and M. Sierra-Pérez, "Electronically reconfigurable transmitarray at Ku band for microwave applications," *IEEE Trans. Antennas Propag.*, vol. 58, no. 8, pp. 2571–2579, Aug. 2010.
[40] J. Y. Lau and S. V. Hum, "Analysis and characterization of a multipole reconfigurable transmitarray element," *IEEE Trans. Antennas Propag.*, vol. 59, no. 1, pp. 70–79, Jan. 2011.
[41] J. Y. Lau and S. V. Hum, "A planar reconfigurable aperture with lens and reflectarray modes of operation," *IEEE Trans. Microw. Theory Techn.*, vol. 58, no. 12, pp. 3547–3555, Dec. 2010.

JESSE BRUNET (Member, IEEE) was born in Arcata, CA, USA. He received the B.S. degree in electrical engineering from the California Polytechnic State University, San Luis Obispo, CA, in 2022, and the M.S. degree in electrical engineering from the California Institute of Technology, Pasadena, CA, in 2024. From 2022 to 2024, he was a Research Assistant with the Caltech Holistic Integrated Circuits (CHIC) Laboratory. Since 2024, he has been with Space Exploration Technologies (SpaceX), Hawthorne, CA. His research interests include antenna theory and design, particularly applied to phased arrays for wireless power transfer and communications. He is a member of Eta Kappa Nu and Tau Beta Pi.

ALEX AYLING (Member, IEEE) received the B.S. degree in electrical engineering from the University of Minnesota, Twin Cities, MN, USA, in 2018, and the M.S. degree in electrical engineering from the University of Illinois, Urbana-Champaign, IL, USA, in 2020. He is currently working toward the Ph.D. degree with the Caltech Holistic Integrated Circuits Laboratory, California Institute of Technology, Pasadena, CA, USA. His research focuses on millimeter-wave and microwave phased-arrays for communications, sensing, and terrestrial/space-based wireless power transfer.

ALI HAJIMIRI (Fellow, IEEE) received the B.S. degree in electronics engineering from the Sharif University of Technology, Tehran, Iran, and the M.S. and Ph.D. degrees in electrical engineering from Stanford University, Stanford, CA, USA, in 1996 and 1998, respectively. He has been with Philips Semiconductors, where he worked on a BiCMOS chipset for GSM and cellular units, and Sun Microsystems, Santa Clara, CA, USA, working on the UltraSPARC microprocessors cache RAM design methodology. During the summer of 1997, he was with Lucent Technologies (Bell Labs), Murray Hill, NJ, USA, where he investigated low-phase-noise integrated oscillators. In 1998, he joined the Faculty of the California Institute of Technology, Pasadena, CA, USA, where he is currently the Bren Professor of Electrical Engineering and Medical Engineering, Director of the Microelectronics Laboratory and Co-Director of the Space Solar Power Project. In 2002, he co-founded Axiom Microdevices Inc., whose fully integrated CMOS PA has shipped around 400 000 000 units, and was acquired by Skyworks Inc., in 2009. He has authored *Analog: Inexact Science, Vibrant Art* (2023, Early Draft) a book on fundamental principles of analog circuit design and *The Design of Low Noise Oscillators* (Springer). He has been granted more than 170U.S. patents with many more pending applications. His research interests include high-speed and high frequency integrated circuits for applications in sensors, photonics, biomedical devices, and communication systems. Dr. Hajimiri is a Fellow of the National Academy of Inventors. He was the recipient of the Feynman Prize for Excellence in Teaching, Caltech's most prestigious teaching honor, and Caltech's Graduate Students Council Teaching and Mentoring Award and the Associated Students of Caltech Undergraduate Excellence in Teaching Award. He was a co-recipient of the IEEE JOURNAL OF SOLID-STATE CIRCUITS Best Paper Award, ISSCC Jack Kilby Outstanding Paper Award, ISSCC Lewis Winner Outstanding Paper Award, RFIC Best Paper Award, and CICC Best Paper Award. He was the Gold Medal Winner of the National Physics Competition and Bronze Medal Winner of the 21st International Physics Olympiad, Groningen, The Netherlands. He was recognized as one of the top-ten contributors to the International Solid-State Circuits Conference (ISSCC). He is the Technology Directions Chair for the Technical Program Committee of the ISSCC and was on the RF and Wireless Committees. He was an Associate Editor for IEEE JOURNAL OF SOLID-STATE CIRCUITS and IEEE TRANSACTIONS ON CIRCUITS AND SYSTEMS–II: EXPRESS BRIEFS, Member for the Technical Program Committee of the International Conference on Computer-Aided Design, and Guest Editor of IEEE TRANSACTIONS ON MICROWAVE THEORY AND TECHNIQUES. He was on the Guest Editorial Board of *Transactions of Institute of Electronics, Information and Communication Engineers of Japan*. He was selected to the TR35 top innovator's list. He was a Distinguished Lecturer for the IEEE Solid-State and Microwave Societies.